scientific reports

Check for updates

OPEN

Dynamic charging behavior of dielectric surfaces induced by electron beam irradiation and its effect on multipacting

Yali Su[1,2]✉, Jiahao Liang[1,2], Dongwei Chen[3], Wenjun Li[3], Xin Zhang[1,2], Dan Wang[4] & Guohe Zhang[4]✉

Spacecraft components working in a complex plasma environment in space environment, and the dielectric modules in the components face the important issue of surface charging. In this work, we quantitatively study the surface potential evolution for dielectrics. The results show that continuous irradiation by the electron beam causes the dielectric surface to reach a balance state, and the balance surface potential is significantly affected by the initial surface potential, the primary electron energy of the incident electrons, and the second critical energy (E_{p2}) of the dielectric. Calculation results show that irradiating uncharged Al_2O_3 sheet continuously with an electron beam of 15,000 eV energy can reach a surface potential of − 9501.01 V, which is a risky high potential. While the balance potential of MgO sheet under the same irradiation condition is only − 1632.34 V, indicating that dielectrics with higher E_{p2} are more favorable for mitigating surface charging. Besides, at electron landing energies below E_{p2}, the surface potentials due to irradiation are too low to induce electrostatic discharge. Multipacting simulations for coaxial filters filled with Al_2O_3 sheets show that the first critical energy (E_{p1}) of the dielectric is affected by the surface potential and further influences the device multipacting threshold. A surface potential of + 20 V/− 80 causes the E_{p1} of Al_2O_3 sheets to drop/increase from 40 eV to 20 V/120 eV, resulting in a decrease/increase in the filter multipacting threshold from 173.4 to 145.3 W/318.4 W. The work is valuable for researching the dynamic charging behavior of dielectric surfaces, and for the engineering application of dielectric multipacting in microwave devices.

Keywords Surface charging, Secondary electron emission, Surface potential, Multipacting

Dielectric surface charging in space environment originates from the interaction between insulating materials and the complex space plasma. When spacecraft components are exposed to charged particles, incident particles penetrate and accumulate within the material due to its low electrical conductivity. Simultaneously, secondary electron emission (SEE) and photoemission further modulate the charge balance[1,2]. Dielectric charging and discharging phenomena in the space environment can lead to a number of reliability problems for the spacecrafts, including electrostatic discharges[2–5], material degradation[6], false telemetry signals, multipacting risks[7,8], electrostatic attraction[9–11]. These effects collectively threaten the reliability of the various spacecrafts.

Among the many scenarios in which dielectric surface charging is induced, the behavior of dielectric surface charging induced by electron irradiation is a very important part. This is not limited to spacecraft environments, in fact, many dielectric surfaces working in plasma environments suffer the charging process induced by electron irradiation, and further face some serious reliability issues. For instances, in Hall thrusters, the SEE phenomenon on the ceramic surface of the discharge cavity BN leads to surface charging, which affects the stability of the plasma in the discharge cavity, as well as the rate at which the ceramic cavity is subjected to ion sputtering[12–15]. In electron multipliers, surface charging affects the multiplication efficiency of the electrodes and may cause reliability problems such as ion feedback[16–18]. In RF systems, charged dielectrics lower the multipacting threshold by enhancing SEE yield, potentially triggering resonant electron avalanches in microwave components like waveguides or filters[19–21]. In reality, multipacting is one of the important mechanism for the performance

[1]School of New Energy, Xi'an Shiyou University, Xi'an 710065, China. [2]Engineering Research Center of Smart Energy and Carbon Neutral in Oil & Gas Field, Universities of Shaanxi Province, Xi'an 710065, China. [3]Tianshui Tianguang Semiconductor Co. Ltd., Tianshui, China. [4]School of Microelectronics, Xi'an Jiaotong University, Xi'an 710049, China. ✉email: sylemon@163.com; zhangguohe@xjtu.edu.cn

degradation or failure of high-power microwave (HPM) components operating in space environment. As well as, multipacting has also received extensive attention in the fields of aerospace microwave equipment, high-energy particle accelerators, and vacuum electronics[22–27]. Unlike multipacting on metal surfaces, the phenomenon of multipacting on dielectric surfaces is significantly affected by charge accumulation. In fact, accumulated charges suppress electron emission barriers, increasing effective SEE yield through field-assisted emission. For example, in 2010, Chang's magnetic suppression study showed SEE yield increases by 0.2–0.5 per 1 kV surface potential on SiO_2, directly lowering multipacting thresholds[28]. Besides, internal charging fields (about 10^6 V/m) vectorially add to RF fields (about 10^4 V/m), creating localized electric field hotspots exceeding dielectric breakdown limits. For instances, in 2005, Sazontov's modeling identified 200% field intensification at material defects under combined fields[29]. Furthermore, time-varying surface potentials during multipacting introduce stochastic phase shifts in electron avalanches. This disrupts traditional susceptibility diagrams, enabling multi-band discharge regions as observed by Rasch in wideband satellite payloads in 2012[30]. In addition, scholars are also committed to studying the process of charge accumulation on dielectric surfaces[31], surface potential evaluation[32,33], surface charge mitigation and charging protection[34], which are all closely related to the SEE process from dielectric surfaces. Based on these discussions, it is essential to investigate the dynamic evolution of surface potential on dielectric materials under electron beam irradiation and its impact on multipacting phenomena, which is crucial for a deeper understanding of multipacting behaviors on dielectric surfaces.

In this work, by analyzing the dielectric surface charging behavior in the case of electron beam incidence with constant energy, the dielectric surface charging process and the final balance state of the system under different conditions are investigated in detail. The influence regularity of the dielectric surface charging on surface potential is calculated and discussed. Besides, the occurrence of the electron multiplication phenomenon is elucidated by evaluating the effect of surface potential on SEE process, and a coaxial filter is employed to evaluate the effect of surface potential on multipacting threshold. The work provides a theoretical basis for the study of the multipacting effect from the dielectric surface charge, and has certain theoretical guidance value for the future exploration of new dielectric surface multipacting suppression methods.

Calculation of surface charging and surface potential

Secondary electron emission leads to surface charging

When the electron beam interacts with the dielectric surface, the effects of many factors need to be considered, such as the electron beam energy, the dielectric surface potential, and environmental factors. Here, the relationship between the outgoing electron flux and the incident electron flux is investigated when the electron beam acts continuously with the dielectric surface. In this process, a constant energy electron beam stream is considered to continuously bombard the dielectric surface, and it is assumed that the electron beams are parallel and there is no energy diffusion. E_p and E_i are employed to represent the primary electron energy and the electron collision energy respectively, the potential of the dielectric surface is denoted as V_i, and e is the elementary charge (-e for single electron). When the electron interacts with the dielectric surface, the following relationship expresses the relationship among the above parameters:

$$E_i = E_p + eV_i \tag{1}$$

It should be noted here that the irradiation induced by ion beam on the dielectric surfaces also induces SEE processes and surface charge accumulation. However, it is well known that the mass of ions is much larger than the mass of electrons, resulting in the specific charge of ions being much smaller than the specific charge of electrons. Therefore the ion flux is much smaller than the electron flux in the usual irradiation scenario, which leads to negligible surface charging induced by ion irradiation compared to the surface charging behavior due to electron irradiation. Therefore, here, we focus our discussion only on the phenomenon of dielectric surface charge accumulation induced by electron irradiation.

After the interaction of electrons with the dielectric surface, there will be three cases: emitting backscattered electrons, emitting secondary electrons, and absorbed by the material, as shown schematically in Fig. 1.

Here, δ and η are employed to be the true secondary electron emission coefficient and the backscattered electron emission coefficient, respectively. The physical meanings of δ and η are the ratio of the number of outgoing true secondary electrons and backscattered electrons to the number of incident electrons, respectively. Then the total electron emission coefficient (TEEY, also denoted as σ), can be expressed as:

$$\sigma = \delta + \eta \tag{2}$$

A typical TEEY curve of neutral dielectric is shown in Fig. 2. There are two special points on the curve making the TEEY equal 1, corresponding to the incident energy E_{p1} (the critical point in the low-energy region, so-called the first critical energy) and E_{p2} (the critical point in the high-energy region, so-called the second critical energy), which satisfy the requirement that the number of electrons emitted is equal to the number of electrons incident. As shown in Fig. 2, the two critical energy points, E_{p1} and E_{p2}, divide the curve into three regions. When $E_{p1} < E_i < E_{p2}$, $\sigma > 1$, the flux of the emitted electron is larger than the flux of the incident electron, indicating that compared with too low or too high incident energy, the incident electron with energy in this energy range can excite more secondary electrons. On the contrary, when $E_i < E_{p1}$ or $E_i > E_{p2}$, $\sigma < 1$, the flux of the emitted electron is smaller than the flux of the incident electron, indicating that too low or too high incident energy will be likely adsorbed by the material bulk, and thus reduce the probability of electron emission from the dielectric surface.

Due to the high insulating properties of the dielectric, when the electron beam interacts with the dielectric surface, the charge induced by SEE cannot flow away in the form of electric current. Then, charge accumulation will be produced on the dielectric surface, and the accumulated charge will induct the corresponding strength

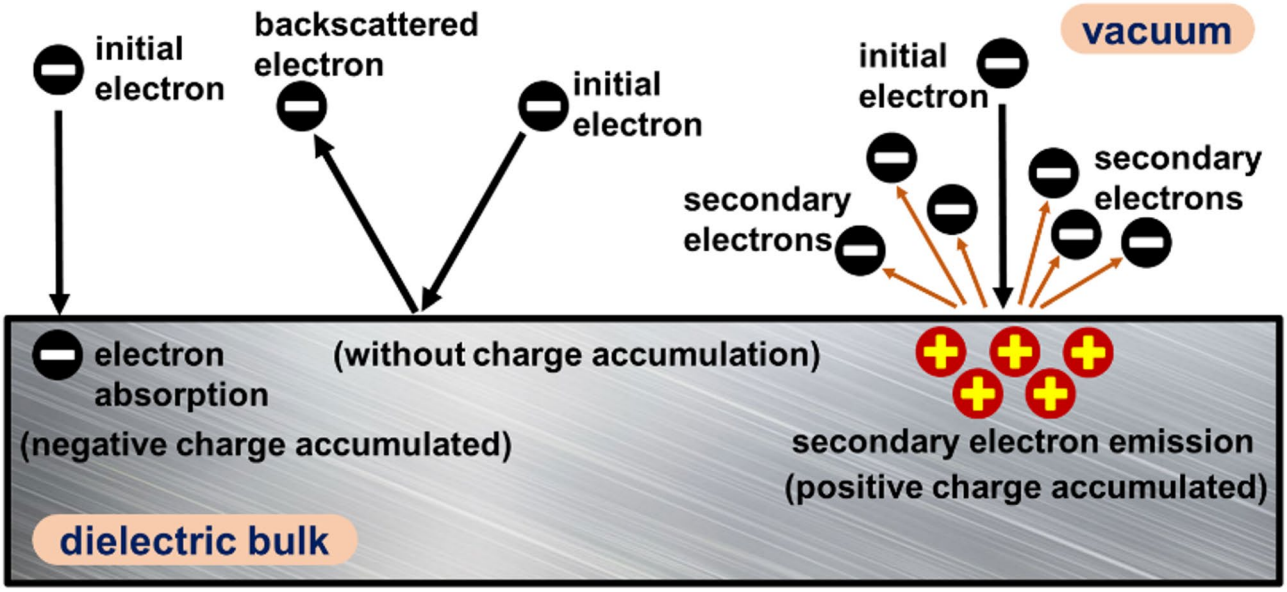

Fig. 1. Interaction between electron and dielectric surface.

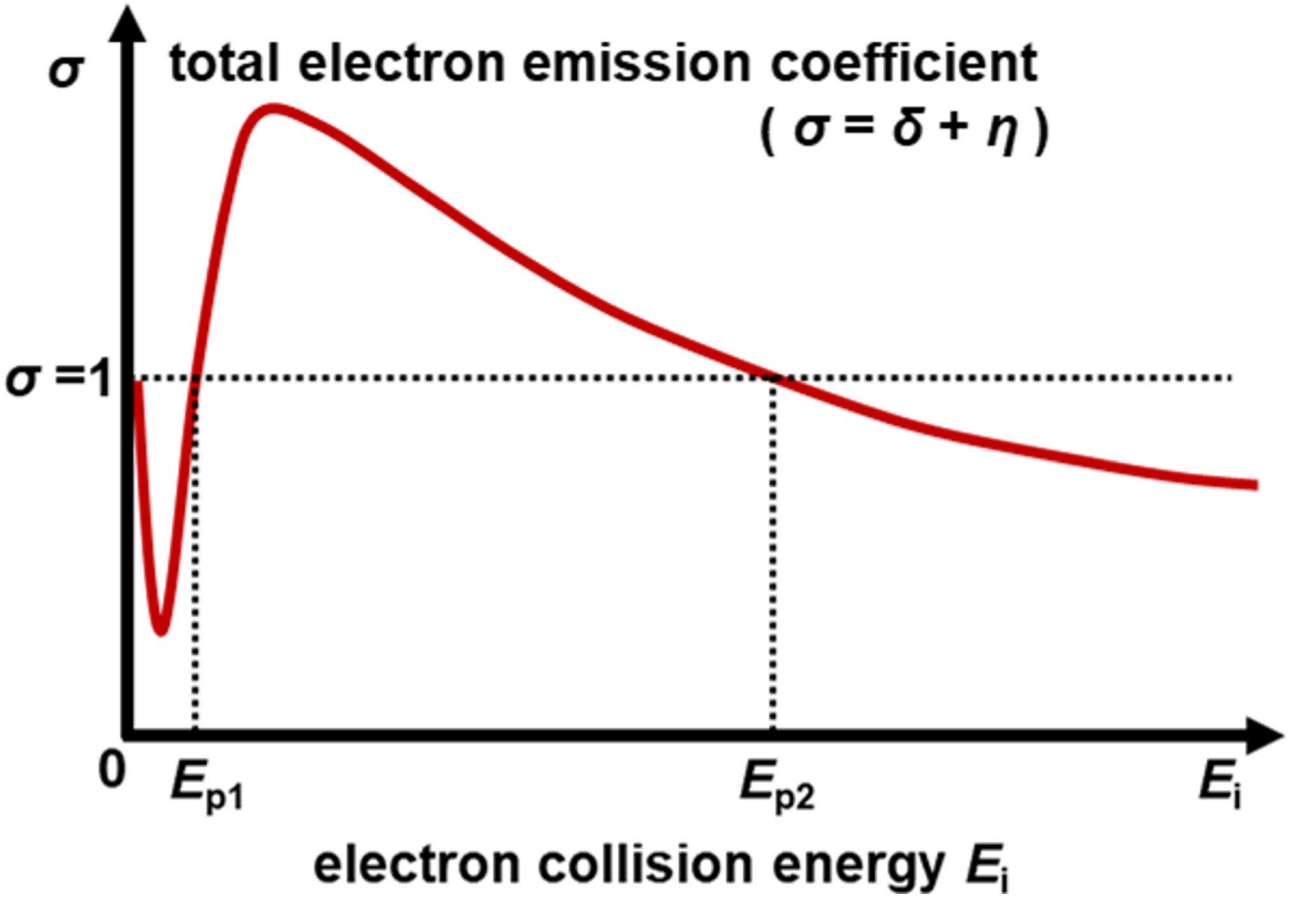

Fig. 2. Typical TEEY curve of dielectric surface without surface charge.

of the electric field, which affects the subsequent energy and trajectory of the incident electrons. When the electron beam collision dielectric surface, there will be secondary electrons and backscattered electrons emitted, and some electrons will be trapped inside the dielectric. In order to reveal the evolution of surface charging in different scenarios, we consider the following three initial potential cases of dielectric surface, uncharged, negatively charged and positively charged (namely $V_i = 0$, $V_i < 0$ and $V_i > 0$), as well as, three kinds of constant energy electron beam flow (namely $E_{p1} < E_i < E_{p2}$, $E_i < E_{p1}$ and $E_i > E_{p2}$) continued bombardment of the dielectric surface. And we are going to discuss the evolution regularity of surface charging and surface potential when the system reaches balance state.

Charge accumulation and surface potential calculations

A theoretical method is used to calculate the surface potential when there is charge accumulation on the dielectric surface. First of all, to give the dynamic process of the dielectric surface potential under electron beam irradiation, it is necessary to know the relationship between the level of charge accumulation and the surface potential. According to the literature[35], when a beam of electron current bombards the surface of a dielectric sample, the level of charge accumulation and the magnitude of the surface potential generated are related to the permittivity, the density of the incident beam current, the TEEY, the size of the beam spot, and the beam action time. Here, J_{in} is set as the incident beam current density, d is the beam spot diameter, ε_0 is the vacuum permittivity with a value of 8.854×10^{-12} F/m, ε_r is the relative permittivity of the dielectric sample, t is the beam current action time with the sample, and Q is the surface charge density. Then the variation of surface charge density, $\Delta Q(t)$, for the dielectric sample after irradiation by the electron beam is reported as:

$$\Delta Q(t) = Q_{\text{in}} - Q_{\text{out}}(t) = J_{\text{in}} t - J_{\text{in}} t \sigma(t) = J_{\text{in}} t \left[1 - \sigma(t)\right] \tag{3}$$

It should be noted in Eq. (3) that the surface potential V_i varies at different moments, as a result, the electron collision energies E_i also varies according to Eq. (1), further leading to the fact that TEEY is also a time-varying parameter. So in Eq. (3), we use $\sigma(t)$ to indicate that TEEY is a time-varying physical parameter. Then the variation of surface potential, $\Delta V_i(t)$, for the dielectric sample is:

$$\Delta V_{\text{i}}(t) = \frac{2d \cdot \Delta Q(t)}{(1 + \varepsilon_r) \cdot \varepsilon_0} \tag{4}$$

If the intensity of the incident beam current is assumed to be I_P, then we have:

$$J_{\text{in}} = \frac{I_{\text{P}}}{\pi \left(d/2\right)^2} = \frac{4 I_{\text{P}}}{\pi d^2} \tag{5}$$

Therefore, the variation of surface potential, $\Delta V_i(t)$ can be calculated by:

$$\Delta V_{\text{i}}(t) = \frac{8 I_{\text{P}} t \left[1 - \sigma(t)\right]}{\pi d (1 + \varepsilon_r) \varepsilon_0} \tag{6}$$

Then the surface charge amount Q and surface potential V_i can be calculated by:

$$Q = \sum \Delta Q \tag{7}$$

$$V_{\text{i}} = \sum \Delta V_{\text{i}} \tag{8}$$

On the basis of the above theoretical Eqs. (3)–(8), it is possible to calculate the charge on the dielectric surface as well as to monitor changes in the surface potential in real time.

Procedure for calculating dielectric surface potentials

To further verify the effect of electron beam irradiation on the surface potential of the dielectric, we carried out the dynamic simulation of the dielectric potential evolution by MATLAB. The calculation of the dielectric surface charge can be carried out in the case of obtaining TEEY fitting curves for the dielectric materials. For the simulations presented in the following section, the irradiation source used was an electron beam stream with the following parameters: the sample was irradiated with a pulsed electron beam stream with a beam intensity of 1×10^{-6} A, a spot diameter of 1×10^{-3} cm, and a duration of a single pulse of 1×10^{-9} s. Two typical dielectrics are chosen as research object, MgO and Al_2O_3. The relative permittivity of MgO is 9.8, and that of Al_2O_3 is 7.2. Here, the experimental TEEY data of MgO and Al_2O_3 in References[36–39] are employed, and the TEEY data of MgO and Al_2O_3 are fitted by the SEE theory developed by Dionne in 1973[40] ensuring that we can compute the TEEY value at any electron collision energy E_i. The flow of surface potential calculation used in the simulation process in the later section is shown in Fig. 3. And the process of calculating the surface potential can be briefly described as follows. At first, set j as the matrix counting unit, for the initial moment, $j = 1$. According to the irradiation energy E_p, surface charge $Q(j)$ and surface potential $V_i(j)$ at $t(j)$ moment, we are able to calculate the electron collision energy $E_i(j) = E_p + eV_i(j)$ at t(j) moment. Based on the dielectric's TEEY curve, we need to judge whether the collision with electron energy of $E_i(j)$ will induce the dielectric positively or negatively charged after SEE process. Then we can calculate the surface charge change ΔQ and surface potential change ΔV_i according to Eqs. (3)–(6) and record $Q(j+1) = Q(j) + \Delta Q$, $V_i(j+1) = V_i(j) + \Delta V_i$ at $t(j+1)$ moment, and so on. After that, we can

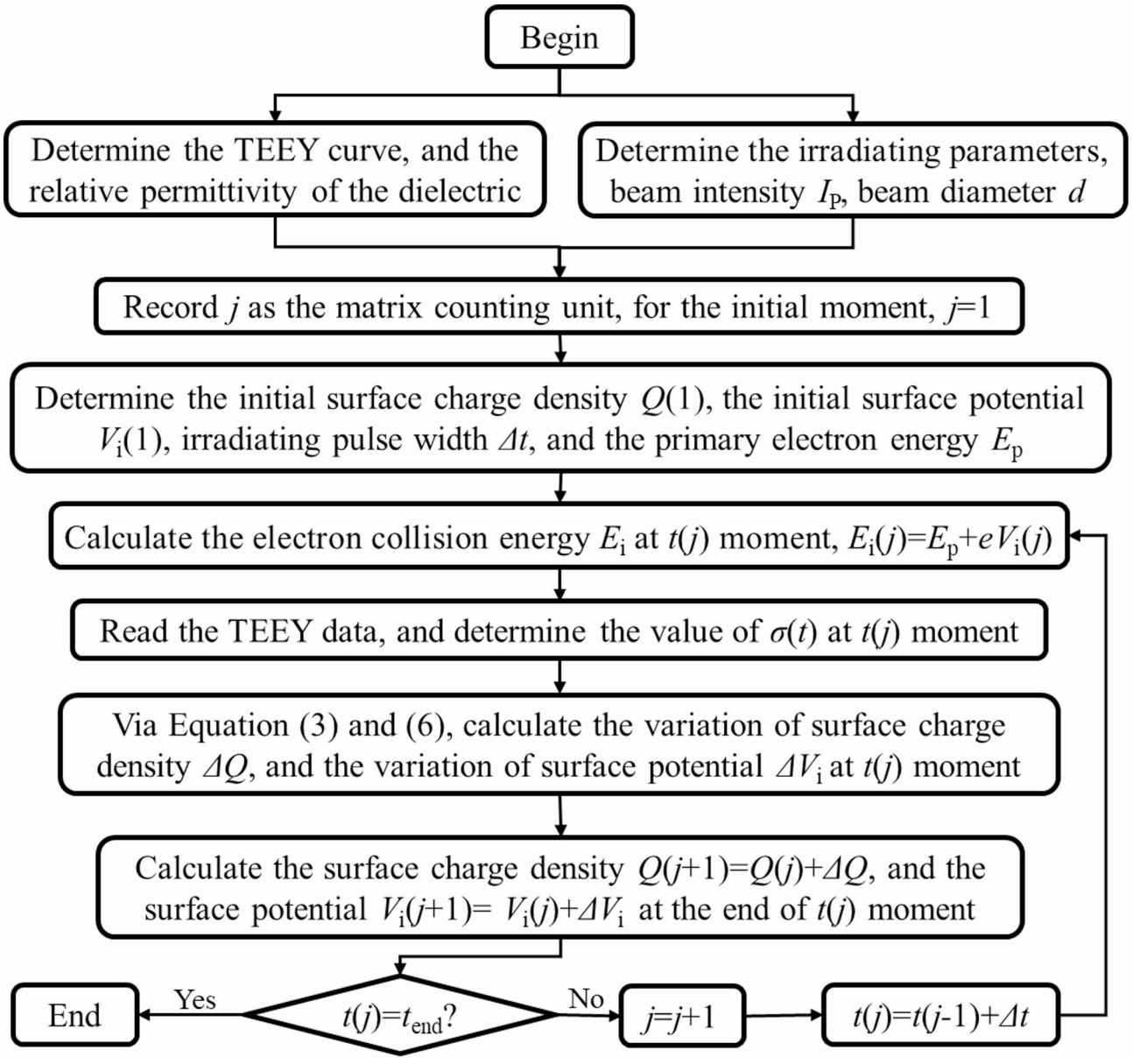

Fig. 3. The flowchart for calculating the surface potential variation process.

calculate the surface charging state at the moment of $t(j+2)$, $t(j+3)$…until the irradiation time $t(j)$ reaches the cut-off value t_{end}. Finally, the surface potential evolution regularity under irradiation time variation is obtained.

It should be noted that for the case of calculating the positively charged surfaces, the attraction of outgoing secondary electrons by the positive surface potential needs to be considered. For example, a positive surface potential of 10 V means that the electrons with energies less than 10 eV cannot escape due to the attraction by the positive surface potential, these electrons are confined on the surface and decrease the positive surface potential. Therefore, when calculating the positive charge cases, firstly, it is necessary to determine the energy distribution of the secondary electrons, and secondly, it is needed to perform a twice calculation of the surface potential in order to obtain the true positive surface potential at a given moment.

Surface charging induced by secondary electron emission

Electron beam collides with uncharged surfaces

When the original surface potential is 0, the dielectric surface is neutral and electron incidence is unaffected. In this case, depending on the energy of the incident electrons, three scenarios occur when electrons continuously bombard the dielectric surface. These three scenarios can be summarized simply in the form of Fig. 4. In the following, we discuss the three scenarios.

If $E_{p1}<E_i<E_{p2}$, the outgoing electron flux is greater than the incident electron flux, the surface potential increases and remains positive, but the typical value of the outgoing secondary electron energy is only a few electron volts, and the number of backscattered electrons is small. At this point, the positive surface charge

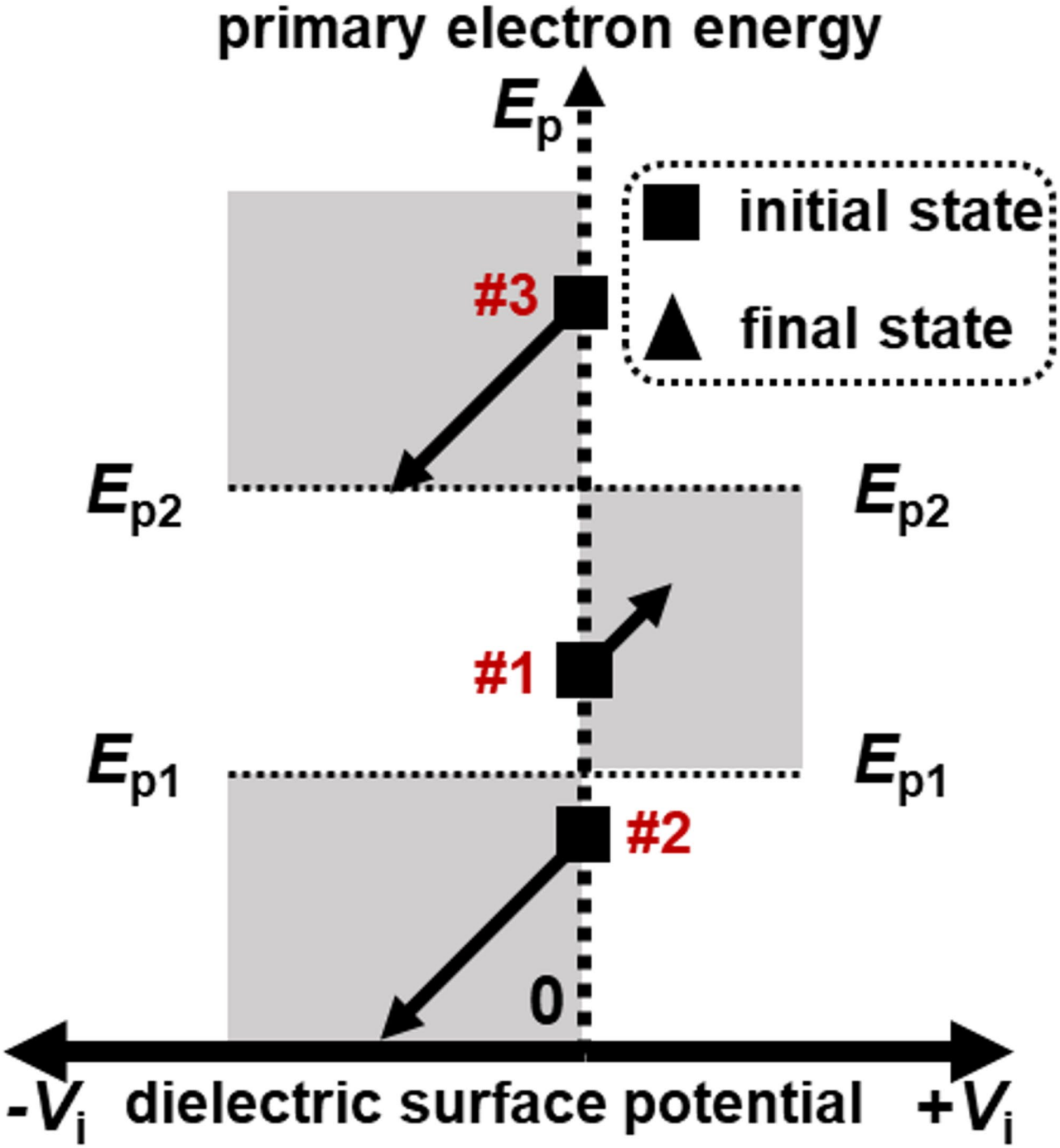

Fig. 4. Three balance scenarios of electron beam bombarding a dielectric surface when the surface potential is 0.

attracts secondary electrons, preventing most of the very low-energy secondary electrons from leaving the dielectric surface. Eventually the above process reaches balance when the surface potential reaches a few positive volts. The final potential of the dielectric surface is stabilized at a few positive volts, and the incident beam current increases the final beam collision energy by a few electron volts as it reaches the surface. In most practical applications, a surface potential of a few volts is not significant and is usually approximated as zero. This scenario corresponds to case #1 in Fig. 4.

If $E_i < E_{p1}$, the outgoing electron flux is less than the incident electron flux, indicating that the surface will produce an electron accumulation, the accumulated electrons make the surface of the dielectric charged to a negative potential. The negatively charged dielectric surface will reduce the collision energy of the incident electron beam, and the collision energy after reduction is still less than E_{p1}, so it will make more electrons accumulate on the dielectric surface. When the dielectric surface charged to a negative potential making the

electron beam collision energy be 0, the process reaches balance, and the final potential of the dielectric surface making the final energy of the beam be a specific negative value. This scenario corresponds to case #2 in Fig. 4.

If $E_i > E_{p2}$, the outgoing electron flux is less than the incident electron flux, the dielectric surface will produce the electron accumulation, and the dielectric surface is so that charged to a negative potential. The negatively charged surface of the dielectric will weaken the energy of the incident electrons, causing the beam collision energy to gradually decrease and approach to E_{p2}. When the negative potential of the dielectric surface continues to increase to a specific value making the final energy of the beam is equal to E_{p2}, then the incident electron flux is equal to the outgoing electron flux, the process reaches balance, the final potential stabilizes at a certain value that makes the beam final energy be E_{p2}. This scenario corresponds to case #3 in Fig. 4.

By using the algorithm in Fig. 3, we calculated the potential evolution when a uncharged dielectric surface is irradiated by an electron beam, results are shown in Fig. 5. V_f in Fig. 5 represents the final surface potential value. Figure 5 reveals that the variation of surface potential is diverse when the electron beam irradiation energy is located in different regions, which is consistent with the analyzed results in Fig. 4. For example, Fig. 5a shows that when the initial electron energy E_p is 40 eV, after several hundred electron pulses of irradiation, the surface potential gradually converges to −40 V which decelerates the incident electron energy to 0. For the case of irradiation-induced positively charged surfaces, the surface potentials of the two dielectrics eventually converge to several tens of V, making the system externally exhibit a TEEY of 1, as shown in Fig. 5b. For the case of electron beam irradiation with higher energy, as shown in Fig. 5c, the magnitude of E_{p2} directly determines the final surface potential, e.g., for electron irradiation with an energy of 15,000 eV, the final surface potential of Al_2O_3 with a small value of E_{p2} is −9451.01 V, while that of MgO with a large value of E_{p2} is only −1632.34 V. This indicates that the dielectric with higher E_{p2} value help to mitigate the surface charging.

Electron beam collides with an initially negatively charged surface

When the original surface potential is negative, the incident electrons are decelerated by the electrical field repulsive force. In this case, depending on the energy of the incident electrons, four scenarios may occur when electrons continuously bombard the dielectric surface. These four scenarios can be summarized simply in the form of Fig. 6, and in the following, we discuss the four scenarios.

If $E_{p1} < E_i < E_{p2}$, the electron outgoing flux is greater than the incident flux, the surface accumulates a positive charge so that the surface potential increases. After continuous bombardment, the final potential of the dielectric surface will return to a few positive volts that making the low-energy secondary electrons not escape, and the final beam collision energy will be a small increase. In this case, the outgoing flux of electrons is equal to the incoming flux, and the system comes to an balance steady state. This scenario corresponds to case #4 in Fig. 6.

Merely, another special balance state exists when $E_{p1} < E_i < E_{p2}$. That is, in the surface positive charge accumulation process, the electron beam collision energy gradually increased. If the potential increase just makes $E_i = E_{p2}$, then the surface potential of the dielectric has not reached enough to confine the low-energy secondary electrons of a few positive volts. However, due to the outgoing electron flux is equal to the incident electron flux in this case, the process has reached balance at this time, the final beam collision energy is E_{p2}, and the ultimate surface potential is a particular value that makes $E_i = E_{p2}$. This scenario corresponds to case #5 in Fig. 6.

If $E_i < E_{p1}$, the incident electron flux exceeds the outgoing electron flux, so that more electrons accumulate on the surface of the dielectric, the surface is charged to a higher negative potential. Due to the effect of the higher negative potential, the energy of the electron beam colliding with the surface decreases. This process will continue until the negative potential increases to a specific value making the collision energy eventually becomes zero, and then the process equilibrates and reaches its final state. This scenario corresponds to case #6 in Fig. 6.

If $E_i > E_{p2}$, the incident electron flux is greater than the outgoing electron flux. As the electron beam continues to bombard the surface of the dielectric, electrons accumulate on the dielectric surface, charging the surface to a higher negative potential, which in turn causes the beam collision energy to decrease. This process will continue until the final beam collision energy E_i is reduced to equal E_{p2}, then the incident electron flux is equal to the

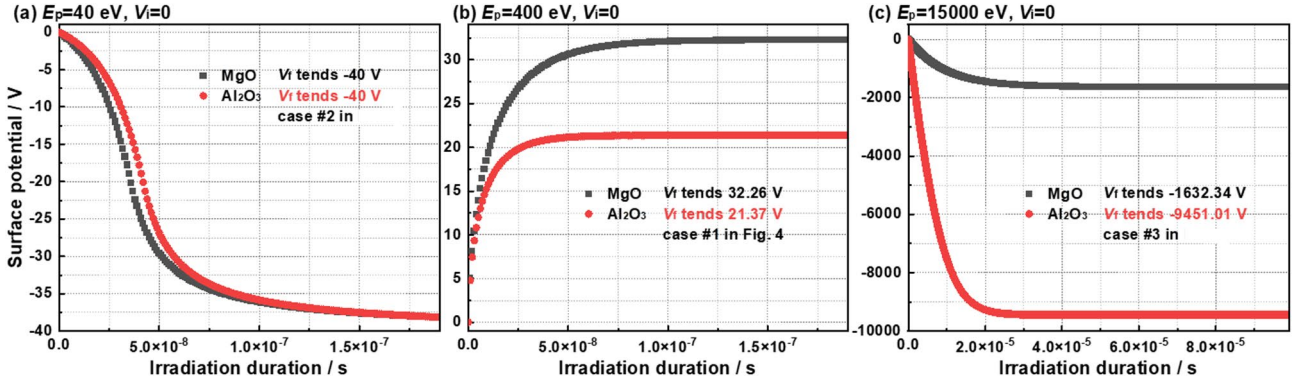

Fig. 5. Surface potential evolution when the dielectric surface is uncharged, (**a**) $E_p = 40$ eV, $V_i = 0$ V; (**b**) $E_p = 400$ eV, $V_i = 0$ V; (**c**) $E_p = 15{,}000$ eV, $V_i = 0$ V.

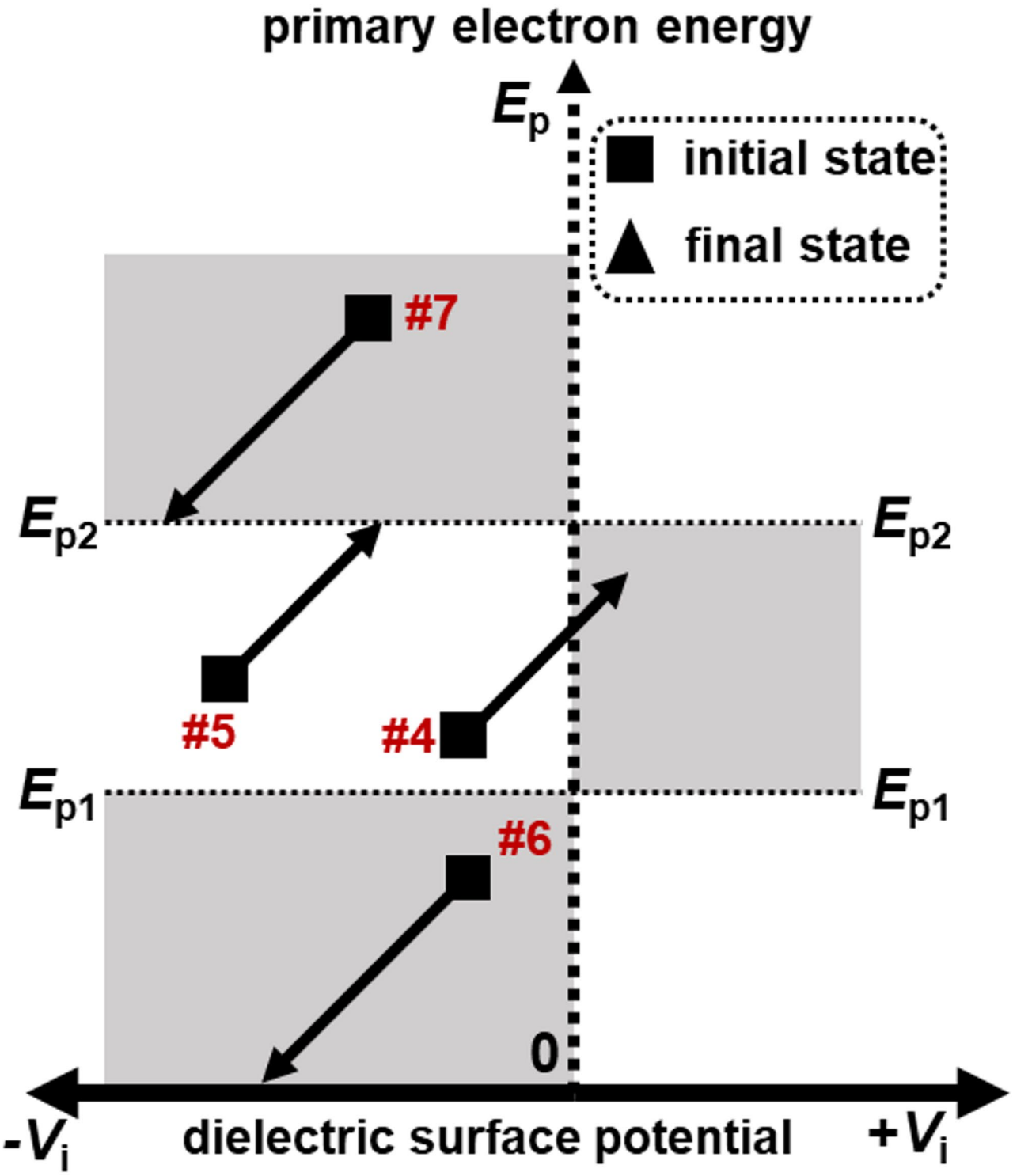

Fig. 6. Four balance scenarios of electron beam bombarding a dielectric surface when the surface potential is negatively charged.

outgoing electron flux, and the potential of the surface will no longer change. In this case, the final potential is a specific value that makes $E_i = E_{p2}$. This scenario corresponds to case #7 in Fig. 6.

Figure 7 shows the surface potential variation when the dielectric is negatively charged, which is consistent with the analyzed results in Fig. 6. The potential evolutions in Fig. 7a,b,d are very similar to the results in Fig. 5a–c, suggesting that the original surface potential in the ordinary case, does not have a significant effect on the potential evolution during the electron beam irradiation. However, the result in Fig. 7c is a special case, if the collision energy of the incident electron beam is between E_{p1} and E_{p2} (more closer to E_{p2}) and the surface

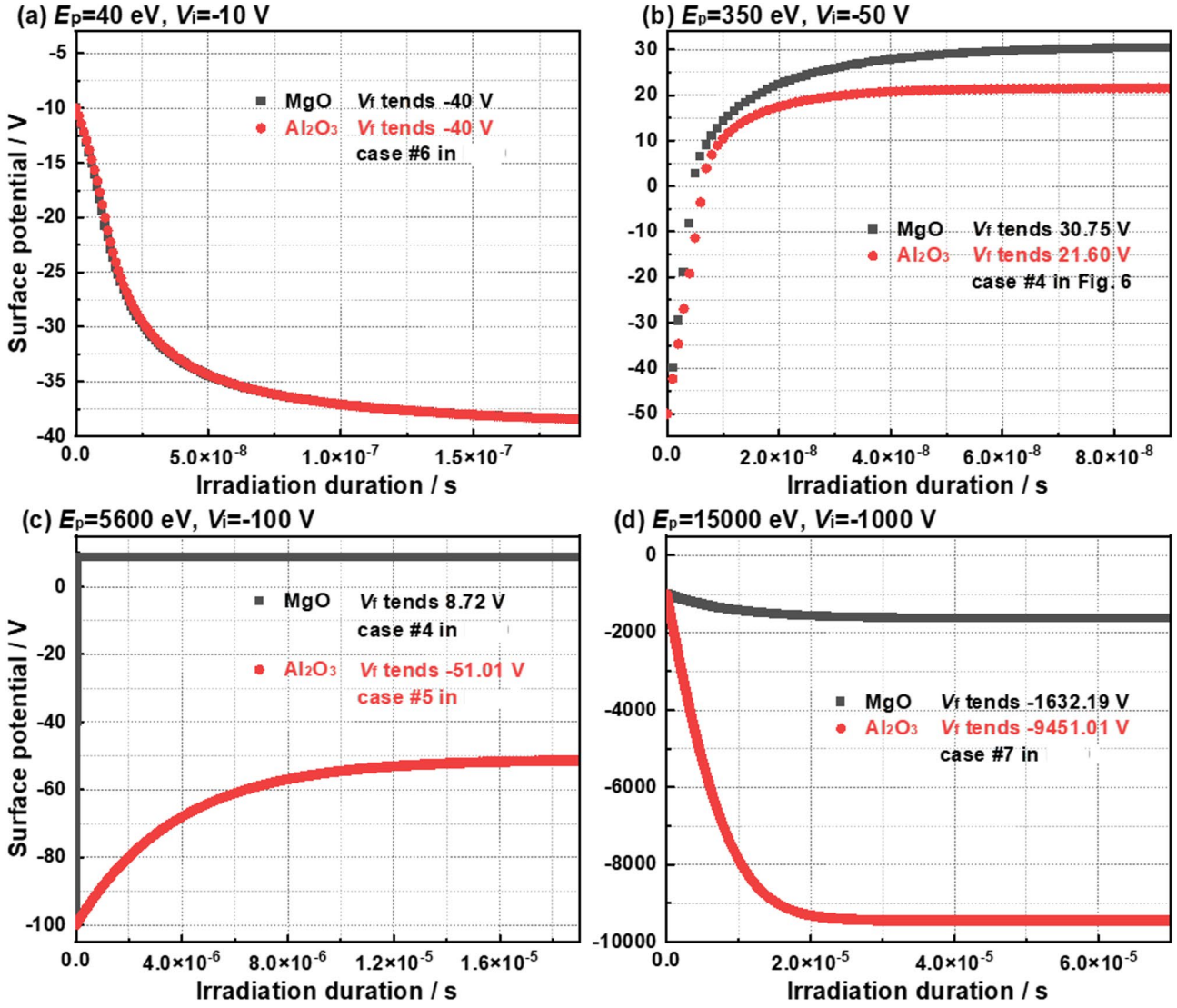

Fig. 7. Surface potential evolution when the dielectric surface is negatively charged, (**a**) $E_p = 40$ eV, $V_i = -10$ V; (**b**) $E_p = 350$ eV, $V_i = -50$ V; (**c**) $E_p = 5600$ eV, $V_i = -100$ V; (**d**) $E_p = 15{,}000$ eV, $V_i = -1000$ V.

negative potential is relatively higher at this time, then the surface negative potential may continue to decrease in this case, and the electron collision energy, E_i, continues to increase until the system reaches a steady state when the electron collision energy E_i is equal to E_{p2}, which corresponds to case #5 in Fig. 6.

Electron beam collides with an initially positively charged surface

When the initial surface potential is positive, the incident electrons are accelerated by the electrical field attraction force. In this case, depending on the energy of the incident electrons, five scenarios may occur when electrons continuously bombard the dielectric surface. These five scenarios can be summarized simply in the form of Fig. 8, and in the following, we discuss the five scenarios.

If $E_{p1} < E_i < E_{p2}$, the TEEY of the surface is greater than 1, the outgoing flux of electrons is greater than the incoming flux. In this case, the positive surface potential of more than a few volts attracts more low-energy secondary electrons back to the surface. As a result, most of the secondary electrons fail to leave the surface because of the attraction of the positively charged surface, and then the surface potential decreases a little. When it comes to the balance state, the final potential will be a few positive volts, and the final beam collision energy will vary depending on the surface potential. This scenario corresponds to case #8 in Fig. 8.

Nevertheless, if E_i continues to decrease to less than E_{p1} with the surface potential being still greater than a few positive volts, the flux of outgoing electrons will be less than the flux of incoming electrons. This case will result in the surface potential continuing to decrease in the direction of the negative potential, and the beam collision energy of the incoming electrons continues to decrease until the final beam collision energy is equal to 0, then the process reaches balance. At this time, the final surface potential of the dielectric for the final beam is a particular value that makes collision energy be 0. This scenario corresponds to case #9 in Fig. 8.

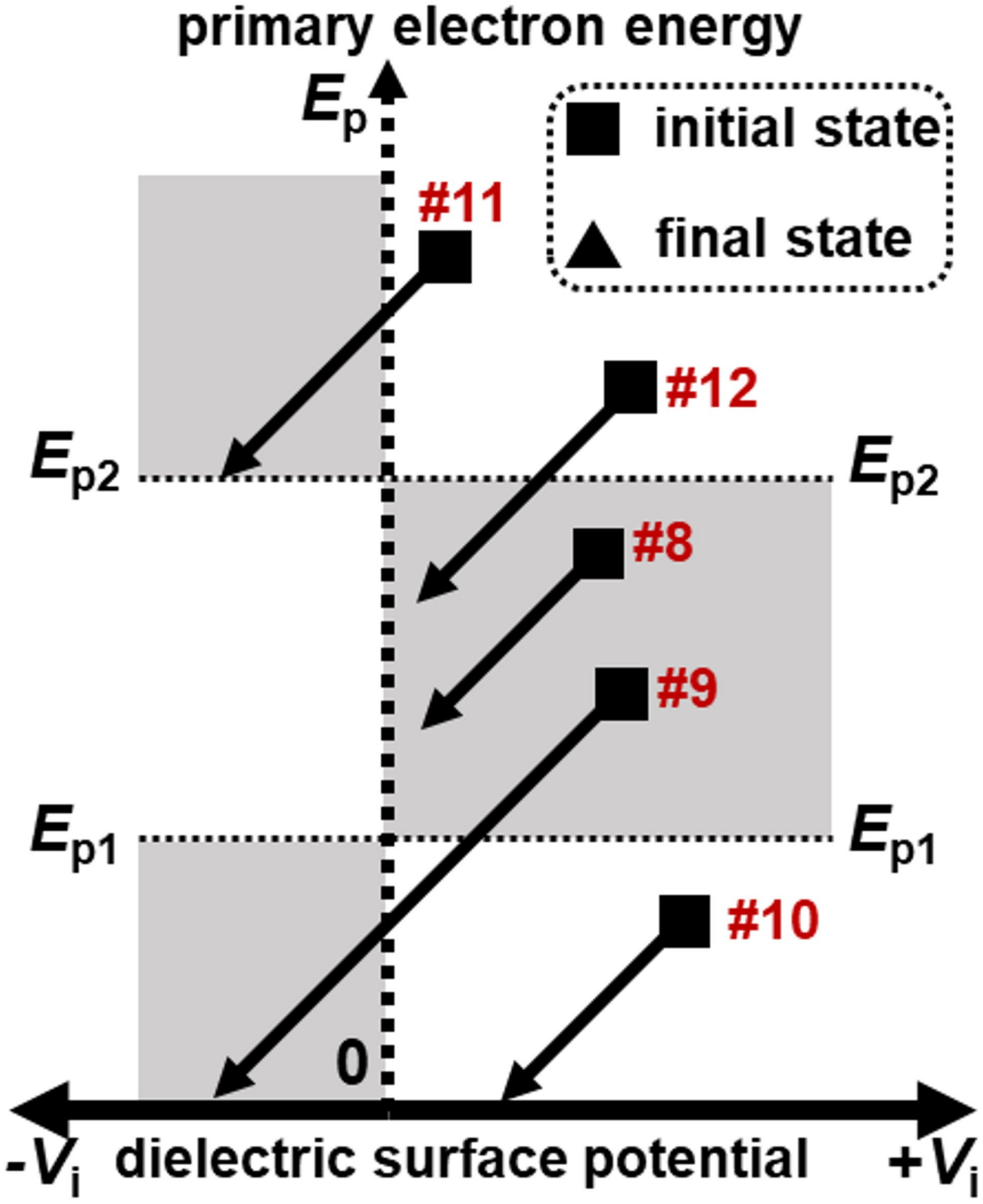

Fig. 8. Five balance scenarios of electron beam bombarding a dielectric surface when the surface potential is positively charged.

If $E_i < E_{p1}$, the flux of outgoing electrons cannot compensate for the flux of incoming electrons, as a result, the surface potential decreases in a negative direction and the beam collision energy continues to decrease. Eventually, the process reaches balance when the beam collision energy is 0, and the final potential of the surface decreases to a specific value that makes the beam collision energy be zero. This scenario corresponds to #10 in Fig. 8.

If $E_i > E_{p2}$, the electron accumulation is achieved on the surface, making the surface potential drop, beam collision energy gradually decreased. The process reaches balance until the beam collision energy is equal to E_{p2}, at which time the final surface potential is a specific value that makes the final beam collision energy equal E_{p2}. This scenario corresponds to case #11 in Fig. 8.

Merely, there is another case for the steady situation of $E_i > E_{p2}$, namely, the initial surface potential of the dielectric is slightly greater than a few positive volts. Under the circumstances, the outgoing electron flux is greater than the incident electron flux, most of the secondary electrons will be confined by the positive charged surface due to their low energy. If the beam energy drops to reach E_{p2}, and the surface potential is still slightly greater than a few positive volts, the process will continue until the surface potential is lower than a few positive volts, close to 0, namely balance state, at which the secondary electrons are able to escape. This scenario corresponds to case #12 in Fig. 8.

Figure 9 shows the surface potential variation when the dielectric is positively charged, which is consistent with the analyzed results in Fig. 8. Here, the potential evolutions in Fig. 9a,b,d are also similar to the results in Fig. 5a,b,c. However, the result in Fig. 9c,e are two special cases. To be specific, if $E_{p1} < E_i < E_{p2}$ (more closer to E_{p1}), the surface potential may continue to decrease in this case, and the electron collision energy, E_i, continues to decrease until the system reaches a steady state when the electron collision energy E_i is 0, which corresponds to case #9 in Fig. 8. If $E_i > E_{p2}$ (more closer to E_{p2}), the surface potential may continue to decrease in this case, and the electron collision energy, E_i, continues to decrease until the surface potential reaches a few positive volts making TEEY = 1, which corresponds to case #11 in Fig. 8.

Overview of surface charging after electron beam collision

From the analysis in Sections "Electron beam collides with uncharged surfaces"–"Electron beam collides with an initially positively charged surface", it can be seen that different surface charging situations as well as initial incident energies will likely lead to different charging behaviors for the dielectric surface. As shown in Fig. 10, the arrows in the Fig. 10 graphically depict the final steady state of the system after the continuous interaction of a single-energy electron beam with the dielectric surface for the 12 initial cases. And in Table 1, we conclude the results of the balance state analysis of the dielectric surface charged in different energy regions. The charging behavior shown in Fig. 10 indicates that the critical energies, E_{p1} and E_{p2}, have significant effects on the charging balance state, but the two critical points have different properties for the system stabilization. For the first critical energies E_{p1}, the beam collision energy at the stabilization time does not stabilize at E_{p1}, no matter how the initial collision energy and the initial surface potential change. However, for the second critical energies E_{p2}, most cases will have a tendency that the final collision energy gradually decreases (or increases) to E_{p2} to achieve the system stabilization. By comprehensive analyzing the charging behavior of the dielectric surface, it shows that the final

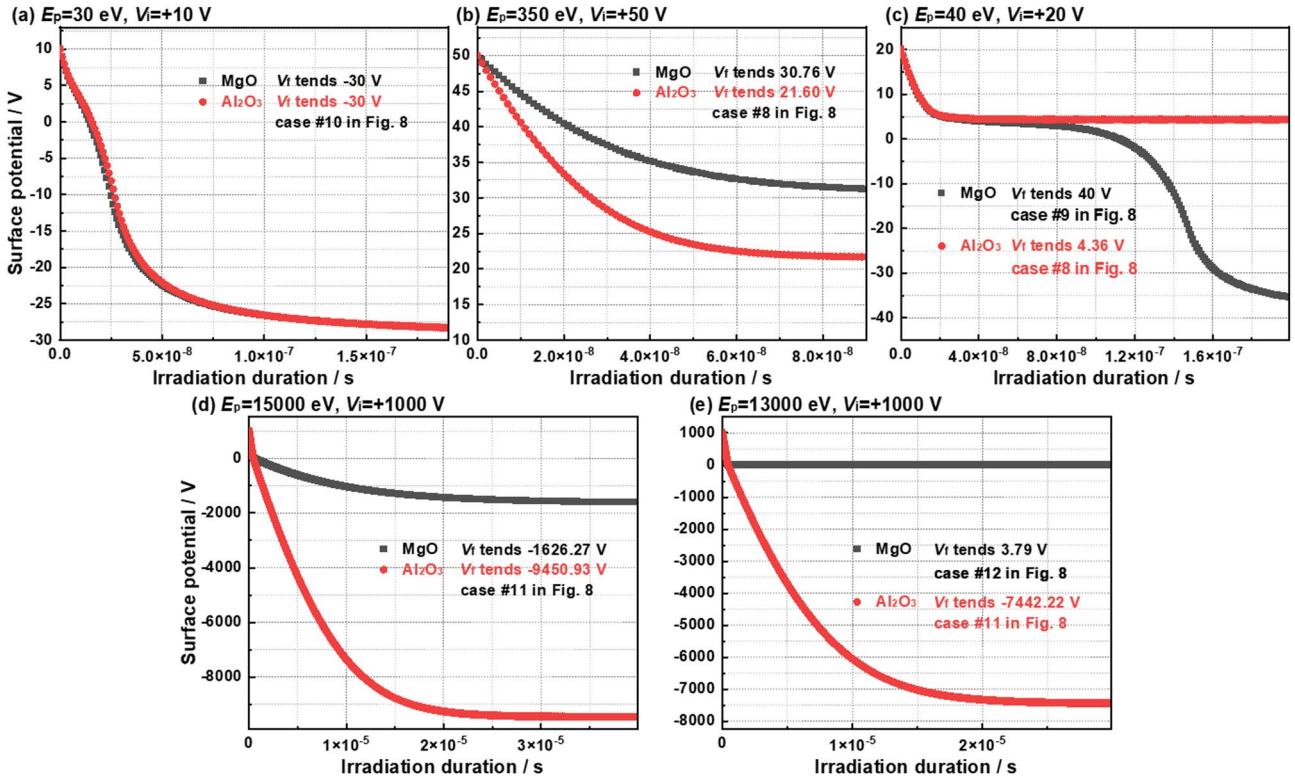

Fig. 9. Surface potential evolution when the dielectric surface is positively charged, (**a**) $E_p = 30$ eV, $V_i = +10$ V; (**b**) $E_p = 350$ eV, $V_i = +50$ V; (**c**) $E_p = 40$ eV, $V_i = +20$ V; (**d**) $E_p = 15{,}000$ eV, $V_i = +1000$ V; (**e**) $E_p = 13{,}000$ eV, $V_i = +1000$ V.

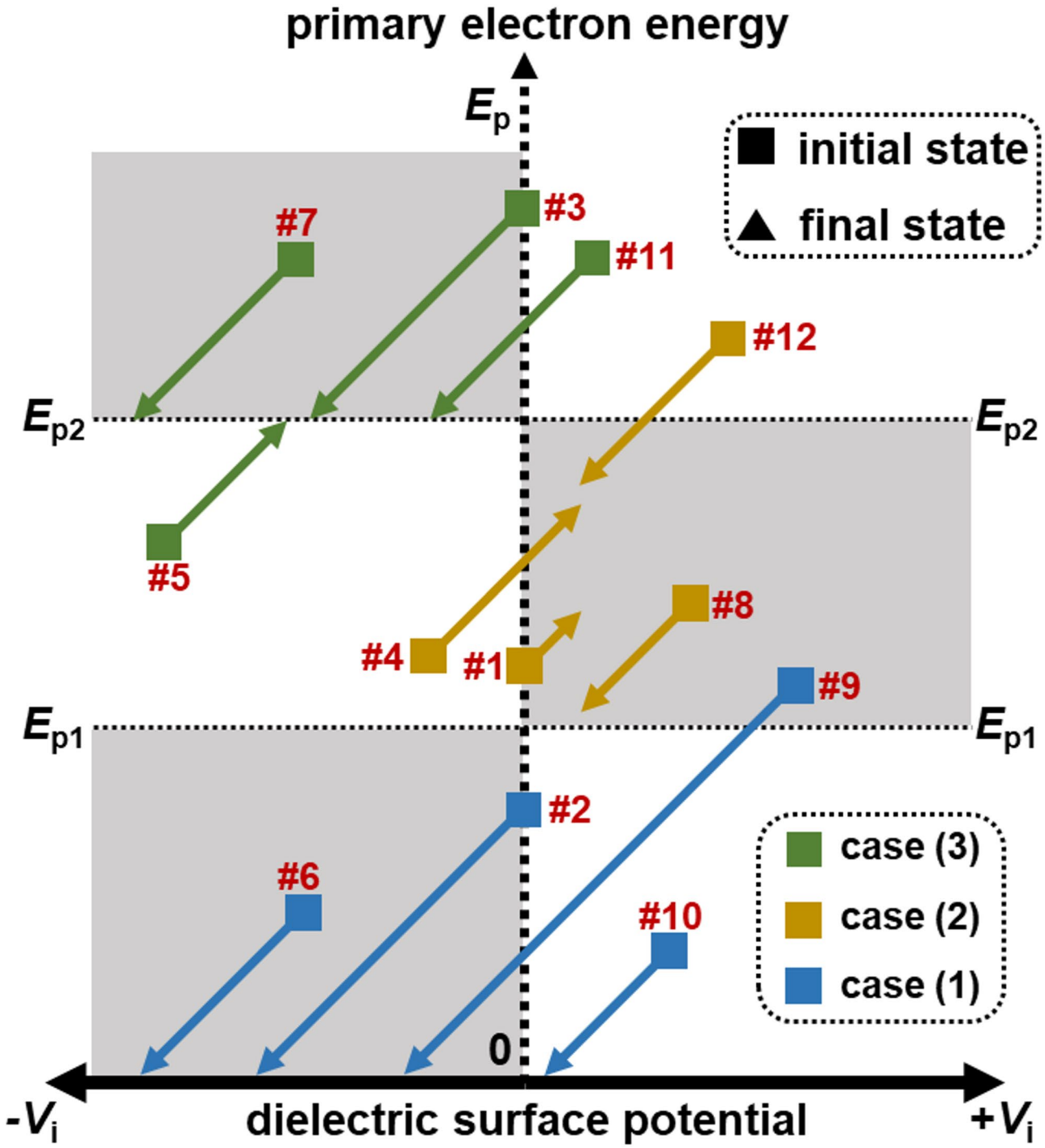

Fig. 10. The summary chart, 12 balance scenarios of electron beam bombarding a dielectric surface when the surface potential is charged in three cases. Case (1), the surface potential reaches a specific value that makes the final beam collision energy 0; Case (2), the surface potential is finally stabilized at a state slightly larger than 0; Case (3), the surface potential equals a specific negative value that makes the final electron beam collision energy be E_{p2}.

stable state of the system can be divided into three types. Case (1), the surface potential reaches a specific value that makes the final beam collision energy 0, this case indicates that there is no electron incidence on the surface, and therefore there is no longer electron ejection and charge accumulation. Case (2), the surface potential is finally stabilized at a state slightly larger than 0 (which can be approximated to be 0), in which case the electrons will be ejected from the surface, but because the ejection energy is very small, it will be taken away by the surface. Since outgoing energy is very small for the most of secondary electrons, they will be attracted by the surface of a small positive potential and cannot escape, forming a state of "confined electron cloud" on the dielectric surface.

Energy region	Irradiation condition: $I_p = 1 \times 10^{-6}$ A, $d = 1 \times 10^{-3}$ cm, $t = 1 \times 10^{-9}$ s			
	Charging type	Potential at balance state	Duration to reach balance state	Discharge risk
$E_p < E_{p1}$	Negative	Dozens of volts	Hundreds of ns	Very low
$E_p > E_{p2}$	Negative	More than thousands volts	Thousands of ns	High
$E_{p1} < E_p < E_{p2}$	Positive	Several volts	Several to dozens of ns	About 0

Table 1. Banlanced process comparision for the dielectric surface potential when the primary electron energy, E_p, locates in various ranges.

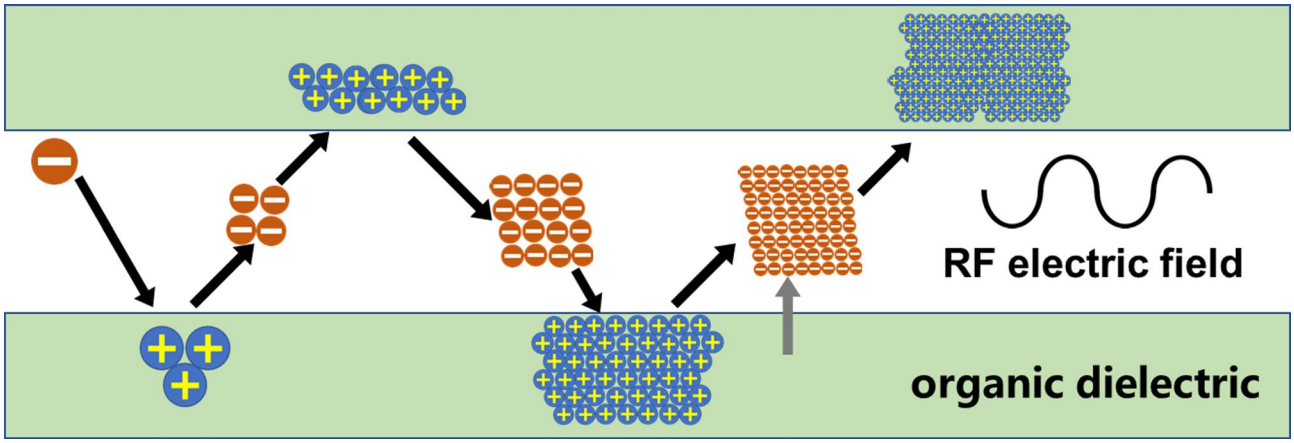

Fig. 11. Electron multiplication between dielectrics under the effect of RF electric field.

Case (3), the surface potential equals a specific negative value that makes the final electron beam collision energy be E_{p2}. The negative surface potential will be accelerated by the ejected electrons so that it is easier to escape, at this time the amount of incident electrons is the same as the amount of and outgoing electrons. Then the system reaches balance, and no further charging and discharging occurs. However, the analysis for Case (3) shows that the final surface potential is determined by the difference between the primary electron energy and E_{p2}, namely, final stable potential equals $(E_p\text{-}E_{p2})/e$. This indicates that a large difference between the primary energy of the electron beam and the surface E_{p2} leads to a high level of charging at the dielectric surface. Therefore for Case (3), dielectrics having high E_{p2} values can reduce the surface charging level. Typically, MgO and Al_2O_3 are two typical dielectrics with high E_{p2} value[36–39], and they may be useful in this regard.

Effect of dielectric surface charging on the multipacting

From the analysis in Section "Surface charging induced by secondary electron emission", it can be seen that different surface initial potentials and collision energies dominate the process of current balance, and also affect the final balance state of the system. In addition, the critical energy and collision energy also show different effects on the system balance. Figure 10 shows that E_{p2} affects the final beam collision energy of the system, while E_{p1}, which is the critical energy for determining TEEY, does not have any significant effect on the system balance. However, E_{p1} is a key factor to determine whether the electrons satisfy the multipacting condition. Here, multipacting on the dielectric surface is qualitatively analyzed by taking the dielectric-filled microwave component as an example. A typical structure of a dielectric-filled microwave component is shown in Fig. 11. In contrast to the double-sided metal plate structure, there is a DC field induced by the charge accumulation on the dielectric surface in addition to the RF field. The two fields simultaneously exert a field force on the particles located between the two plates. Compared with a single electric field, the energy and trajectory of particles (including initial electrons and secondary electrons) under the action of the double electric field are not only affected by the electromagnetic wave, but also by the electrostatic field produced by the surface charge, and thus the surface charge must affect the threshold of the occurrence of multipacting on the surface of the dielectric.

Constant energy electron beam incident dielectric surface

The TEEY is a key indicator of whether or not the multipacting effect can occur, in addition to the resonance conditions. Multiplication at resonant conditions is only possible if the incident electron beam on the collision surface produces a TEEY greater than 1. Here we consider the electron beam with constant energy incident on the dielectric surface, and evaluate the influence of the surface potential on multipacting for dielectric surface in the case of low-energy and high-energy electron incidence respectively.

Influence of surface potential on E_{p1}

When the incident energy of electrons is low (around E_{p1}), the size of the critical energy in the low-energy region, which makes the TEEY of 1, determines the threshold conditions for the occurrence of the multipacting. When the electron interacts with the surface of the dielectric, there exists a specific primary function relationship between the initial energy of the electron, the collision energy, the charge and the primary surface potential, just as described in Eq. (1). If it is assumed that the initial electron energy E_p is equal to the first critical energy E_{p1}, consider the magnitude of the collision energy in the two cases of negatively and positively charged initial dielectric surface, respectively: (i) If $V_i<0$, $E_i=E_p+eV_i<E_p$, $E_i<E_{p1}$, non-balance, $\sigma<1$; (ii) if $V_i>0$, $E_i=E_p+eV_i>E_p$, $E_i>E_{p1}$, non-balance, $\sigma>1$.

It is worth noting that the surface potential V_i in the above scenarios do not change the electron energy too much. In other words, the following two scenarios are neglected: (1) $V_i<<0$, the electrons are so strongly repelled by the surface potential that they cannot reach the dielectric surface; (2) $V_i>>0$, the electrons are so strongly attracted by the surface potential making $E_i>E_{p2}$. From the above analysis, it can be seen that in the case when the dielectric surface is negatively charged, $V_i<0$, there is an obvious repulsive force on the electrons, and the electron collision energy decreases compared to the initial energy. From another perspective, we can consider the surface potential makes E_{p1} increase to $E_{p1}+eV_i$. Since the energy range of $\sigma<1$ is extended, we can consider that the negatively charged surface is more conducive to inhibit the occurrence of the multipacting effect on the dielectric surface. When the dielectric surface is positively charged, $V_i>0$, the change in electron energy is just opposite. Positively charged dielectric surface for the electron has an attractive force, the electron collision energy compared to the initial energy increased, from the perspective of the change, it can be considered that the first critical energy, E_{p1}, has been reduced, and at this time there is a TEEY is greater than 1 to meet the conditions of electron multiplication, there is a risk of generating multipacting effect.

Influence of surface potential on E_{p2}

Similar analysis can also be applied to the surface potential on the influence of the law. If it is assumed that the initial energy of the electron is equal to the second critical energy E_{p2}, consider the magnitude of the collision energy in the two cases of negatively and positively charged initial dielectric surface, respectively: (i) If $V_i<0$, $E_i=E_p+eV_i<E_p$, $E_i<E_{p2}$, non-balance, $\sigma>1$; (ii) if $V_i>0$, $E_i=E_p+eV_i>E_p$, $E_i>E_{p2}$, non-balance, $\sigma<1$.

From the above analysis, it can be seen that in the case of the negatively charged surface of the dielectric, the collision energy of the electrons compared to the initial energy decreases when the surface has a significant repulsive force on the electrons. From the perspective of E_{p2} change, if the assumption that the collision energy of the electron is the initial energy, it can be considered that E_{p2} was raised to $E_{p2}+eV_i$. In this case, the TEEY is greater than 1, which meets the conditions of the electron multiplication. On the contrary, when the surface of the dielectric is positively charged, it has an accelerating effect on the electrons, the electron collision energy compared to the initial energy increased. At this time, the TEEY is smaller than 1, there is no risk of generating multipacting effect.

Continuous energy electron beam incident on the dielectric surface

The considerations in Section "Constant energy electron beam incident dielectric surface" are based on a case of constant electron beam energy irradiation. However, in the actual space environment, the energy of the space particle beam changes all the time. The result of the space charged beam interacting with the dielectric surface is often a superposition of the above states, including the effect on the dielectric surface potential, E_{p1}, E_{p2}, and the final collision energy of the electron beam. It is worth noting that although the surface potential affects the critical energy, the energy range that makes the TEEY greater than 1 does not change. When the surface of the dielectric is negatively or positively charged, E_{p1} and E_{p2} are increased or decreased by eV_i, and this change has a significant effect on multipacting occurrence.

If the energy of the incident electron beam is continuous, the effect of surface charging on the multipacting is significantly different from that of a constant electron beam incident. Here we assume that the energy of the incident electron beam is continuous and its quantity is uniformly distributed between the upper and lower energy limits, and set E_x and E_y as the upper and lower limits of the energy region, respectively. By dividing the result of the integration using the TEEY of a particular energy interval by the width of the energy interval, we can obtain the average TEEY within that energy interval. Here we integrate the SEE curves from E_x to E_y, and we set the integration result of the interval (E_x, E_y) to be Y, and the average electron emission coefficient to be y, then there exists the following relationship between Y and y:

$$y = \frac{Y}{E_y - E_x} \tag{9}$$

Considering that parameter y is a statistical physical quantity, if $y<1$, then the electrons do not multiply and do not satisfy the conditions for multipacting, and conversely if $y>1$ then there is a risk of multipacting. In this case, if a certain potential exists at the surface, the upper and lower limits of the electrons are shifted in the same direction by an equal amount, as shown in Fig. 12. Here, we set the following parameters: when there is no surface potential, the total integral area of the interval (E_x, E_y) is Y; when there is surface potential, the total integral area of the interval (E_x+eV_i, E_y+eV_i) is Y_0, and at this time, the resulting integral area offsets at E_x and E_y are Y_x and Y_y, respectively. Besides, σ_{max} is the maximum of TEEY, and E_{pmax} is the E_p corresponding to σ_{max}.

Effect of negative surface potential

When the surface potential is negative, E_x and E_y are shifted to the left, and for the integral increase, at this time, there is a relationship between Y_0 and Y as follows:

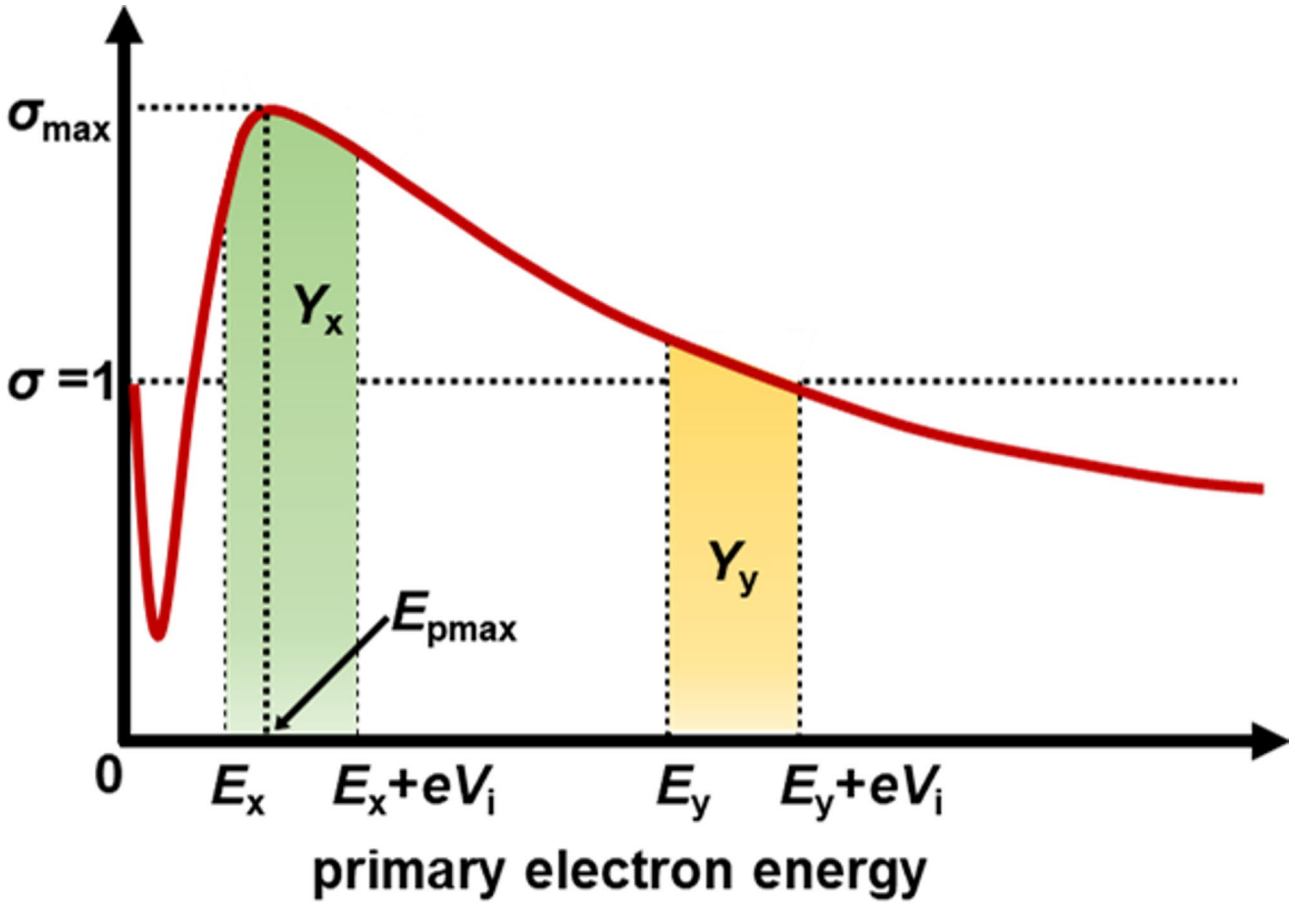

Fig. 12. Electron energy shifting induced by surface potential.

$$Y_0 = Y + Y_x - Y_y \tag{10}$$

Considering that there is no risk of multipacting if $Y_0 < 1$, the following discussion does not take into account the case that makes $Y_0 < 1$.

(i) If $E_y < E_{pmax}$, then $Y_x < Y_y$, according to Eq. (8), $Y_0 < Y$, and the risk of multipacting is reduced.
(ii) If $E_x > E_{pmax}$, then $Y_x > Y_y$, makes $Y_0 > Y$, and the risk of multipacting is increased.
(iii) If $E_x < E_{pmax} < E_y$, then there are three possibilities, namely, $Y_x < Y_y$, $Y_x > Y_y$, and $Y_x = Y_y$. In this case, according to Eq. (10), the change of the Y_0 depends on the relationship between the area of Y_x and Y_y. At this time, if $Y_x > Y_y$, then Y_0 increases, the risk of occurrence of multipacting increases; vice versa, the risk of the occurrence of multipacting decreases.

Effect of positive surface potentials
When the surface potential is positive, E_x and E_y are shifted to the right, and for the integral increase, at this time, there is a relationship between Y_0 and Y as follows:

$$Y_0 = Y - Y_x + Y_y \tag{11}$$

In this case, there are also three cases (the following discussion does not consider the case that makes $Y_0 < 1$):

(i) If $E_y < E_{pmax}$, then $Y_x < Y_y$, according to Eq. (9), $Y_0 > Y$, and the risk of multipacting is increased.
(ii) If $E_x > E_{pmax}$, then $Y_x > Y_y$, makes $Y_0 < Y$, and the risk of multipacting is decreased.
(iii) If $E_x < E_{pmax} < E_y$, then there are three possibilities, namely, $Y_x < Y_y$, $Y_x > Y_y$, and $Y_x = Y_y$. In this case, according to Eq. (11), the change of the Y_0 depends on the relationship between the area of Y_x and Y_y. At this time, if $Y_x > Y_y$, then Y_0 decreases, the risk of occurrence of multipacting decreases; vice versa, the risk of the occurrence of multipacting increases.

The above analyses show that the dielectric surface charging will largely change the energy range of the incident electron beam, thus affecting the occurrence of multipacting. In this process, the average electron emission coefficient, Y_0, is an important indicator of the occurrence of multipacting, as well as the increase or decrease of multipacting risk.

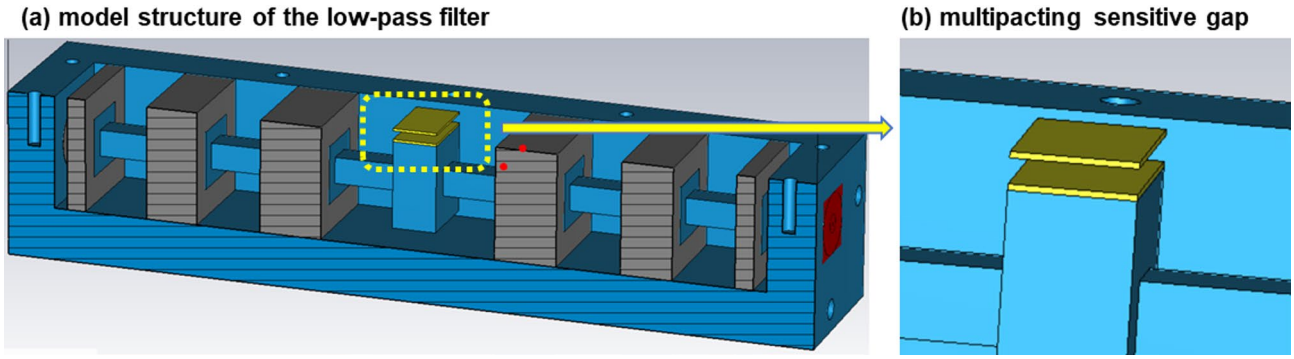

Fig. 13. Multipacting simulation device, a 5 GHz coaxial low-pass filter model.

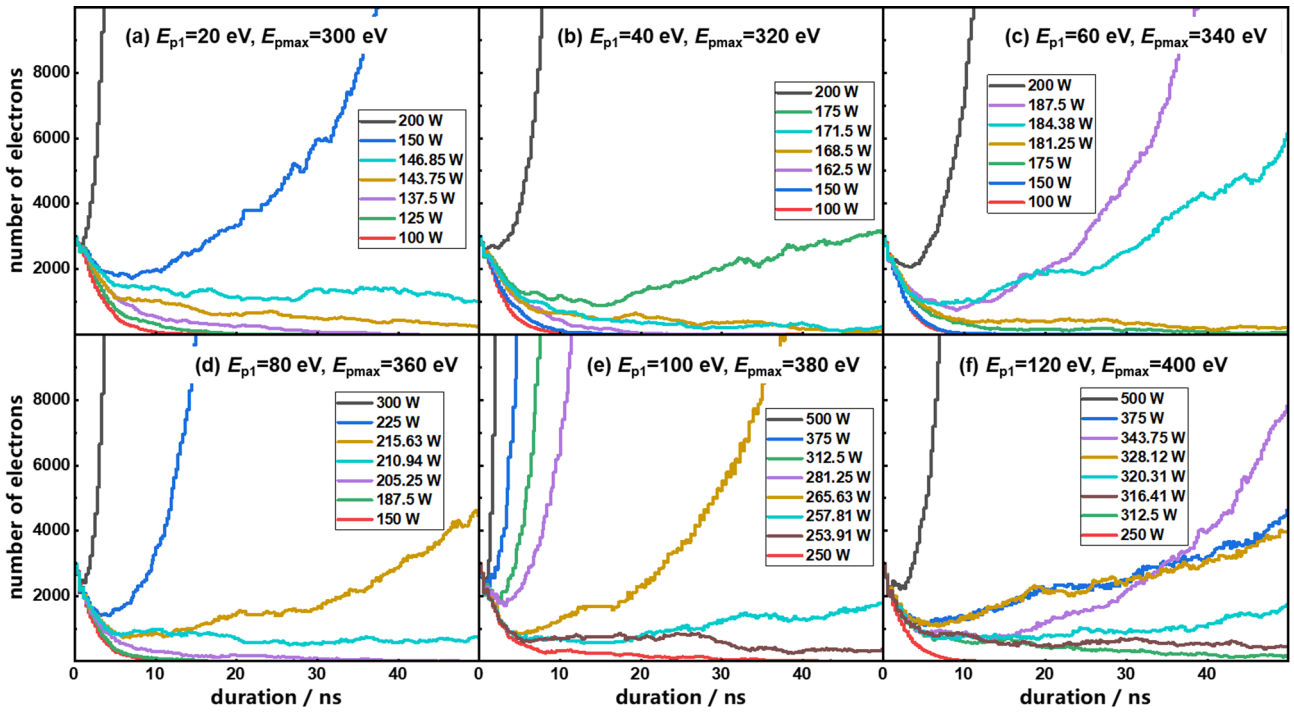

Fig. 14. Simulation results of the electron number evolution with different E_{p1} values, (**a**) E_{p1} = 20 eV, (**b**) E_{p1} = 40 eV, (**c**) E_{p1} = 60 eV, (**d**) E_{p1} = 80 eV, (**e**) E_{p1} = 100 eV, (**f**) E_{p1} = 120 eV.

Effect of surface potential on multipacting

The above discussion shows that dielectric surface charging has a significant effect on TEEY, next we discuss the effect of surface charging on multipacting. Here, to investigate the effect of dielectric charging on multipacting, we apply a low-pass filter as the study object, as shown in Fig. 13. The device model was built by Vague et al.[41]. The centermost part of the device was filled with two alumina dielectric sheets. The gap width between the two alumina sheets is 1 mm, which is the most multipacting prone gap structure in the device. Before the simulation, the device model built in CST needs to be imported into SPARK3D. Then the simulation area is defined, and the parameters such as material TEEY data, input power, number of seed electrons and solution accuracy are set. After the above settings are finished, the simulation is started, and the variation of the electron number with duration is obtained under different parameter values. During the simulation, the TEEY peak value, σ_{max}, of the alumina sheet was kept at 4.3 and the number of seed electrons was set to 3000. Depending on the level of surface charging, we set the value of E_{p1} in the TEEY curve from 20 to 120 eV.

Figure 14 illustrates the results of the electron number evolution with microwave power duration. Here, by observing the simulation results of the electron number evolution corresponding to the six sets of E_{p1} values, we are able to extract the multipacting threshold values of the low-pass filter, as shown in Table 2. The simulation results show that the multipacting threshold of the filter is 173.4 W when the alumina surface is not charged, at which time the E_{p1} value corresponding to the TEEY curve of the alumina sheet is 40 eV. When the alumina surface is positively charged, the electron landing energy increases, which can be relatively considered as a

Surface potential (V)	+ 20	0	− 20	− 40	− 60	− 80
E_{p1} value (eV)	20	40	60	80	100	120
Multipacting threshold (W)	145.3	173.4	182.8	208.6	255.9	318.4

Table 2. Simulated multipacting threshold values of the low-pass filter when the alumina surface is charged in various potential.

decrease in E_{p1}. For example, when the surface potential is + 20 V, it can be considered that E_{p1} decreases by 20 eV, at which point the simulation yields a filter multipacting threshold of only 145.3 W. On the contrary, if the alumina surface is negatively charged, the incident electrons are repulsed by the surface potential, resulting in a decrease in the landed energy, and it can be relatively considered that the value of E_{p1} increases. For example, when the surface potential is − 40 V, it can be considered that E_{p1} increases by 40 eV to 80 eV, at which time the simulation obtains the multipacting threshold of the filter is raised to 208.6 W. When the negative surface potential rises to − 80 V, E_{p1} increases by 80 eV to 120 eV, at which time the simulation obtains the multipacting threshold of the filter is raised to 318.4 W. From the above analysis, it is clear that the negatively charged alumina surface contributes to the increase in E_{p1} value, which leads to an increase in the multipacting threshold for the alumina-filled region in the filter as well.

Conclusion

In this work, we have analyzed the evolution of the surface potential and electron collision energy of a dielectric irradiated by an electron beam of constant energy. The conditions for the irradiation system to reach balance, as well as the electron collision energy and the surface potential of the dielectric at balance, are derived from the analyses and calculations. In addition, by using a bilateral ideal dielectric as an example, we have analyzed the effect of surface charging on the critical energy of TEEY and the probability of occurrence of multipacting. Two important conclusions can be drawn from the analyses in this work, as follows. (1) When the dielectric surface is irradiated with low energy electrons (less than E_{p1}), the system will eventually make the collision electron beam energy converge to 0; in the case of high energy electrons (more than E_{p2}) irradiation, the system will eventually make the collision electron beam energy converge to E_{p2}. (2) Charging of the dielectric surface due to electron irradiation induces a shift in the incident electron beam energy, which causes a change (higher or lower) in the average TEEY corresponding to the energy range in which the beam is located, which further affects the probability of multipacting occurring on the surface of the bilateral dielectric under the RF field (higher or lower). The work is of engineering significance for quantifying the surface charging state of dielectric surfaces in the space environment, and is of guidance value for improving the protection level of space dielectrics against electric charges.

Data availability

The datasets used and/or analyzed during the current study available from the corresponding author on reasonable request.

Received: 23 March 2025; Accepted: 16 June 2025
Published online: 01 July 2025

References

1. Lai, S. T. *Fundamentals of Spacecraft Charging* (Princeton University Press, 2011).
2. Koons, H. C., Mazur, J. E., Selesnick, R. S., et al. (2000). The impacts of the space environment on space systems. In *Proceedings of the 6th Spacecraft Charging Conference*, 7–11. Hanscom.
3. Lian, Z. X. et al. Surface potential evolution and DC discharge measurement of the microstrip antenna dielectric under electron beam irradiation. *Vacuum* **138**, 114270 (2025).
4. Garrett, H. B. & Whittlesey, A. C. Spacecraft charging, an update. *IEEE Trans. Plasma Sci.* **28**(6), 2017–2028 (2000).
5. Garrett, H. B. & Close, S. Impact-induced ESD and EMI/EMP effects on spacecraft—A review. *IEEE Trans. Plasma Sci.* **41**(12), 3545–3557 (2013).
6. Lian, Z. X. et al. Discharge characteristics of the planar microscale gap electrodes with various geometry structures in the atmosphere environment. *Results Phys.* **62**, 107823 (2024).
7. Vaughan, J. R. M. Multipactor. *IEEE Trans. Electron Devices* **35**(9), 1172–1180 (1988).
8. Seviour, R. The role of elastic and inelastic electron reflection in multipactor discharges. *IEEE Trans. Electron Devices* **52**(9), 1927–1930 (2005).
9. Cho, M. (2007). Charging and discharge in vacuum and space. In *Proceedings of IEEE International Vacuum Electronics Conference*, 1–4. Kitakyushu.
10. Gupta, S. B. et al. An overview of spacecraft charging research in India: Spacecraft plasma interaction experiments—SPIX-II. *IEEE Trans. Plasma Sci.* **42**(5), 1072–1077 (2014).
11. Tafazoli, M. A study of on-orbit spacecraft failures. *Acta Astronaut.* **64**(2–3), 195–205 (2009).
12. Gu, Y. Q., Li, J. N. & Wang, D. Investigation on the electron emission regularity of sputtered boron nitride thin films and microstructured array surfaces. *Inorganics* **13**, 102 (2025).
13. Lian, Z. X. et al. Secondary electron emission reduction from boron nitride composite ceramic surfaces by the artificial microstructures and functional coating. *J. Phys. D Appl. Phys.* **57**(31), 315304 (2024).
14. Khartov, S. A. & Shkarban, I. I. Investigation of promising ceramic materials in discharge chambers of stationary plasma thrusters. *Russ. Aeronaut.* **51**(3), 382–387 (2008).
15. Tondu, T., Belhaj, M. & Inguimbert, V. Electron-emission yield under electron impact of ceramics used as channel materials in Hall-effect thrusters. *J. Appl. Phys.* **110**(9), 093301 (2011).

16. Va'vra, J. & Sumiyoshi, T. Ion feedback suppression using inclined MCP holes in a "single-MCP plus micromegas plus pads" detector. *Nuclear Instrum. Methods Phys. Res. Sect. A Accel. Spectrometers Detectors Assoc. Equip.* **553**(1–2), 76–84 (2005).
17. Lian, Z. X. et al. High-performance microchannel plates based on atomic layer deposition for the preparation of functional layers. *J. Phys. D Appl. Phys.* **58**(11), 115106 (2025).
18. Sauli, F., Kappler, S. & Ropelewski, L. Electron collection and ion feedback in GEM-based detectors. *IEEE Trans. Nucl. Sci.* **50**(4), 803–808 (2003).
19. Kishek, R. A. et al. Multipactor discharge on metals and dielectrics: historical review and recent theories. *Phys. Plasmas* **5**(5), 2120–2126 (1998).
20. Kishek, R. A. & Lau, Y. Y. Multipactor discharge on a dielectric. *Phys. Rev. Lett.* **80**(14), 3198–3200 (1998).
21. Meng, X. C. et al. Secondary roughness effect of surface microstructures on secondary electron emission and multipactor threshold for PTFE-filled and PI-filled single ridge waveguides. *J. Phys. D Appl. Phys.* **57**(26), 265301 (2024).
22. Wang, D. et al. Ultralow electron emission yield achieved on alumina ceramic surfaces and its application in multipactor suppression. *J. Phys. D Appl. Phys.* **55**(45), 455301 (2022).
23. Semenov, V. E. et al. General study of multipactor between curved metal surfaces. *IEEE Trans. Plasma Sci.* **42**(3), 721–728 (2014).
24. Arregui, I. et al. High-power low-pass harmonic filters with higher-order, and non-mode suppression: Design method and multipactor characterization. *IEEE Trans. Microw. Theory Tech.* **61**(12), 4376–4386 (2013).
25. Anza, S. et al. Prediction of multipactor breakdown for multicarrier applications: the quasi-stationary method. *IEEE Trans. Microw. Theory Tech.* **60**(7), 2093–2105 (2012).
26. Sinitsyn, O., Nusinovich, G. & Antonsen, T. Studies of multipactor in dielectric-loaded accelerator structures: Comparison of simulation results with experimental data. *AIP Conf. Proc.* **1299**(1), 302–306 (2010).
27. Mori, S., Yoshida, M. & Satoh, D. Multipactor suppression in dielectric-assist accelerating structures via diamondlike carbon coatings. *Phys. Rev. Accel. Beams* **24**(2), 022001 (2021).
28. Chang, C. et al. Suppression of high-power microwave dielectric multipactor by resonant magnetic field. *Appl. Phys. Lett.* **96**(11), 111502 (2010).
29. Sazontov, A. et al. Effect of emission velocity spread of secondary electrons in two-sided multipactor. *Phys. Plasmas* **12**(11), 113310 (2005).
30. Rasch, J. & Johansson, J. F. Non-resonant multipactor—A statistical model. *Phys. Plasmas* **19**(12), 123101 (2012).
31. Wang, F., Qiu, Y., Pfeiffer, W. & Kuffel, E. Insulator surface charge accumulation under impulse voltage. *IEEE Trans. Dielectr. Electr. Insul.* **11**(5), 847–854 (2004).
32. Bekkeng, T. A. et al. Multi-needle langmuir probe system for electron density measurements and active spacecraft potential control on cubeSats. *IEEE Trans. Aerosp. Electron. Syst.* **55**(6), 2951–2964 (2019).
33. Wang, J. Y. et al. Dynamic evolution investigation on the dielectric surface charging under electron irradiation with various energy distributions. *Results Phys.* **57**, 107339 (2024).
34. Lai, S. T. A critical overview on spacecraft charging mitigation methods. *IEEE Trans. Plasma Sci.* **31**(6), 1118–1124 (2003).
35. Braga, D. et al. Secondary electron emission yield on poled silica based thick films. *J. Appl. Phys.* **96**, 885–894 (2004).
36. Lian, Z. X. et al. Effect of atmospheric environment on the stability of secondary electron emission from magnesium oxide and alumina surfaces. *J. Phys. D Appl. Phys.* **57**(12), 125302 (2024).
37. Suharyanto, et al. Secondary electron emission and surface charging evaluation of alumina ceramics and sapphire. *IEEE Trans. Dielectr. Electr. Insul.* **13**(1), 72–78 (2006).
38. Choi, E. H. et al. Secondary electron emission coefficient of a MgO single crystal. *J. Appl. Phys.* **86**(11), 6525–6527 (1999).
39. Prodanovic, V. et al. Effect of thermal annealing and chemical treatments on secondary electron emission properties of atomic layer deposited MgO. *J. Vac. Sci. Technol. A* **36**(6), 06A102 (2018).
40. Dionne, G. F. Effects of secondary electron scattering on secondary emission yield curves. *J. Appl. Phys.* **44**, 5361–5364 (1973).
41. Vague, J. et al. Multipactor effect characterization of dielectric materials for space applications. *IEEE Trans. Microw. Theory Tech.* **66**, 3644 (2018).

Author contributions

Yali Su: Conceptualization; Investigation; Data curation; Formal analysis; Methodology; Writing-original draft; Software. Jiahao Liang: Investigation; Methodology; Writing-original draft. Dongwei Chen: Writing, Reviewing and Editing; Project administration; Methodology. Wenjun Li: Visualization; Validation; Writing-review & editing. Xin Zhang: Writing-review & editing; Methodology; Conceptualization. Dan Wang: Validation; Investigation; Writing-original draft; Writing-review & editing. Guohe Zhang: Writing-review & editing; Software; Data curation; Formal analysis; Resources; Methodology; Project administration; Investigation.

Funding

This work was supported by the National Key Research and Development Program of China under Grant 2023YFB2504100, the Natural Science Foundation of Gansu Province, China (Grant No. 23ZDGE001), and the Natural Science Foundation of Shaanxi Province, China (Grant No. 2024JC-YBMS-525).

Declarations

Competing interests

The authors declare no competing interests.

Additional information

Correspondence and requests for materials should be addressed to Y.S. or G.Z.

Reprints and permissions information is available at www.nature.com/reprints.

Publisher's note Springer Nature remains neutral with regard to jurisdictional claims in published maps and institutional affiliations.